

# An “Enhanced PET”-Based Fluorescent Probe with Ultrasensitivity for Imaging Basal and Elesclomol-Induced HClO in Cancer Cells

Hao Zhu,<sup>†</sup> Jiangli Fan,<sup>\*,†</sup> Jingyun Wang,<sup>‡</sup> Huiying Mu,<sup>†</sup> and Xiaojun Peng<sup>\*,†</sup>

<sup>†</sup>State Key Laboratory of Fine Chemicals and <sup>‡</sup>School of Life Science and Biotechnology, Dalian University of Technology, Dalian 116024, China

**S** Supporting Information

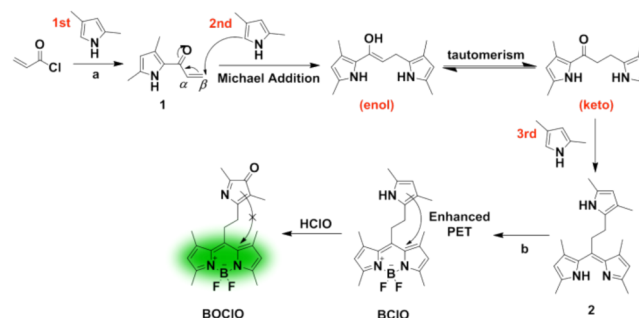
**ABSTRACT:** Reactive oxygen species (ROS) and cellular oxidant stress have long been associated with cancer. Unfortunately, the role of HClO in tumor biology is much less clear than for other ROS. Herein, we report a BODIPY-based HClO probe (BCIO) with ultrasensitivity, fast response (within 1 s), and high selectivity, in which the pyrrole group at the *meso* position has an “enhanced PET” effect on the BODIPY fluorophore. The detection limit is as low as 0.56 nM, which is the highest sensitivity achieved to date. BCIO can be facilely synthesized by a Michael addition reaction of acryloyl chloride with 2,4-dimethylpyrrole and applied to image the basal HClO in cancer cells for the first time and the time-dependent HClO generation in MCF-7 cells stimulated by elesclomol, an effective experimental ROS-generating anticancer agent.

Reactive oxygen species (ROS), such as H<sub>2</sub>O<sub>2</sub>, HClO, HO•, RO<sub>2</sub>•<sup>-</sup>, and <sup>1</sup>O<sub>2</sub>, are constantly generated and eliminated in biological systems; they play important roles in diverse normal biochemical functions and abnormal pathological processes.<sup>1</sup> In particular, ROS and cellular oxidant stress have long been associated with cancer.<sup>2</sup> Growing evidence suggests that cancer cells in general exhibit increased intrinsic ROS stress compared to normal cells.<sup>3–5</sup> The cancer cells depend on a high ROS level to drive proliferation and other events required for tumor progression.<sup>2</sup> However, further oxidative stress may exhaust the cellular antioxidant capacity and increase the ROS stress beyond the threshold level, leading to apoptosis,<sup>6,7</sup> which is considered as a novel anticancer mechanism,<sup>1,2,8</sup> such as that of elesclomol.<sup>9</sup> That is, ROS is a double-edged sword for cancer cells. O<sub>2</sub>•<sup>-</sup> and H<sub>2</sub>O<sub>2</sub> have been shown to be implicated in oncogenic transformation,<sup>5</sup> while actually much of the H<sub>2</sub>O<sub>2</sub> generated by neutrophils is used to produce hypochlorous acid (HClO) by myeloperoxidase (MPO).<sup>10,11</sup> Unfortunately, the role of HClO in tumor biology is much less clear.<sup>12</sup>

Under physiological conditions, HClO is highly reactive and short-lived;<sup>13</sup> the average level of HClO generation from neutrophils is 0.47 nmol/min per 10<sup>6</sup> cells.<sup>14</sup> HClO detection with fast response and high sensitivity is desirable for real-time monitoring of the fluctuation of HClO in its cellular site of action. Although several efforts have been made to develop HClO-responsive fluorescent probes,<sup>15–35</sup> most of them display a delayed response time, and no example is sensitive enough to report on the basal HClO level in cancer cells. Herein, we report a fluorescent BODIPY-based HClO probe, BCIO

(Scheme 1), with ultrasensitivity (detection limit of 0.56 nM), high selectivity, and fast response (within 1 s). The

## Scheme 1. Synthesis and Proposed HClO Sensing Mechanism of BCIO<sup>a</sup>



<sup>a</sup>Reagents and conditions: (a) CH<sub>2</sub>Cl<sub>2</sub>, rt, overnight; (b) NEt<sub>3</sub>, BF<sub>3</sub>·OEt<sub>2</sub>, rt, 2 h, 11.3%.

excellent sensing properties of BCIO enable its use in the imaging of basal HClO in cancer cells for the first time and the real-time monitoring of HClO generation in MCF-7 cells stimulated by elesclomol.

Probe BCIO was constructed by connecting a difluoroboron dipyrromethene (BODIPY) fluorophore and a 2,4-dimethylpyrrole moiety acting as the recognition group through a two-carbon linker. It was facilely synthesized by a Michael addition reaction of one acryloyl chloride molecule with three 2,4-dimethylpyrrole molecules (Scheme 1). Pyrrole is an aromatic five-membered heterocycle and the nonbonding electrons on the pyrrole nitrogen overlay with the π system to form a continuous ring.<sup>36</sup> We envisioned that, compared with the traditional single-atom electron donor (O, N,<sup>37,38</sup> Se,<sup>22,35,39,40</sup> Te,<sup>34,41</sup> etc.) for photoinduced electron transfer (PET), the more electron-rich pyrrole ring can “switch off” the fluorescence of fluorophore more efficiently through an “enhanced PET” effect which gives lower background fluorescence and higher signal-to-noise ratio. When the pyrrole is oxidized by HClO to its corresponding keto form (BOCIO), the fluorescence can be restored because of the suppression of PET (Scheme 1).

The spectroscopic properties of BCIO (1 μM) were evaluated in an aqueous medium buffered to physiological

Received: June 14, 2014

Published: August 29, 2014

pH (0.01 M PBS, ethanol/water = 1:9 v/v, pH 7.4). Free **BCIO** featured a prominent absorption band centered at 500 nm ( $\epsilon = 7.1 \times 10^4 \text{ M}^{-1} \text{ cm}^{-1}$ ) and a corresponding emission maximum at 505 nm with weak fluorescence ( $\Phi = 0.006$ ), as expected. Upon addition of NaClO, almost no change in the absorption spectrum was observed (Figure S1). However, the emission of **BCIO** was enhanced by approximately 100-fold in intensity and 56-fold in quantum yield ( $\Phi = 0.347$ ) with 5  $\mu\text{M}$  NaClO added (Figure S2). The low background fluorescence and large enhancement, which are ascribed to “enhanced PET” by the pyrrole ring, make **BCIO** superior to the majority of other PET-based probes.<sup>22,34,37–39</sup> In the selectivity test, other ROS ( $\text{H}_2\text{O}_2$ ,  $\text{O}_2^{\bullet-}$ , TBHP,  $\text{HO}^\bullet$ ,  $\text{TBO}^\bullet$ ,  $^1\text{O}_2$ , NO) at higher concentrations did not lead to measurable changes in the fluorescence of **BCIO** (Figure 1d). The high-resolution mass

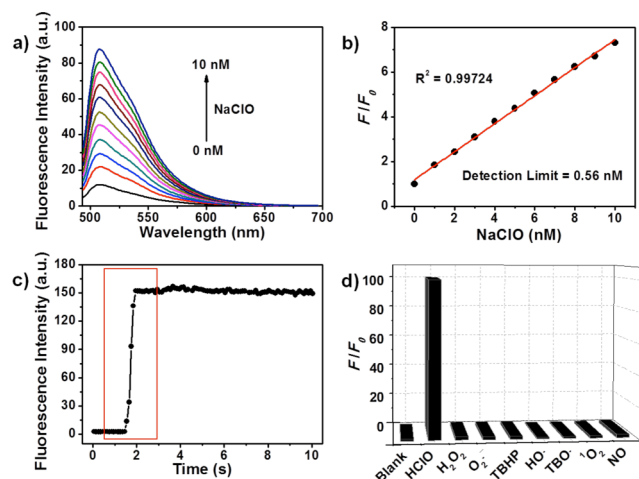


**Figure 1.** Spectroscopic properties of **BCIO** (1  $\mu\text{M}$ ) in PBS (0.01 M) solution (ethanol/water = 1:9 v/v, pH 7.4). (a) Fluorescence spectra and (b) intensity ratios ( $F/F_0$ , 505 nm) of **BCIO** change as a function of NaClO (at 0–10 nM). (c) Time course of fluorescence intensity of **BCIO** at 505 nm after addition of 5  $\mu\text{M}$  NaClO, time range 0–10 s. (d) Fluorescence responses ( $F/F_0$ , 505 nm) of **BCIO** toward NaClO (5  $\mu\text{M}$ ) and other ROS (10  $\mu\text{M}$ ). The excitation wavelength is 480 nm.

spectrum (HRMS) of **BCIO**+HClO (Figure S3) showed two signals at  $m/z$  406.1871 (calcd 406.1873) and 789.3860 (calcd 789.3853), which could be assigned to  $[\text{BCIO}+\text{Na}]^+$  and  $[2\text{BCIO}+\text{Na}]^+$ , respectively. Infrared (IR) spectroscopic analysis (Figure S4) showed that a distinct IR absorption peak at  $1710 \text{ cm}^{-1}$  corresponding to the C=O group appeared upon the addition of NaClO to **BCIO**. The fluorescence signal output of **BCIO** with HClO was clarified in terms of the frontier orbital energy diagrams by the density functional theory (DFT) method at the B3LYP/6-31G(d,p) level using the Gaussian 09 program (Figure S5). Furthermore, the redox potentials of the BODIPY fluorophore and 2,4-dimethylpyrrole were measured by differential pulse voltammetry (DPV), which ascertained the PET mechanism in **BCIO** (Figure S6).

To examine the sensitivity of **BCIO** to HClO, titration of HClO at low concentrations was conducted. As shown in Figure 1a,b, the fluorescence intensity ratio ( $F/F_0$ , 505 nm) of **BCIO** was linearly proportional ( $R^2 = 0.99724$ ) to the HClO concentration in the range 0–10 nM. Importantly, the detection limit was calculated to be as low as 0.56 nM ( $3\sigma/k$ ). To the best of our knowledge, this is the highest HClO sensitivity achieved for fluorescent probes to date.<sup>20,35</sup> The

time-dependent fluorescence changes (at 505 nm) of **BCIO** in the presence of NaClO (Figure 1c and Figure S7) showed that the reaction can be completed within 1 s. Indeed, the short response time is essential for the real-time detection of HClO. The pH titration experiment (Figure S8) revealed that **BCIO** maintained a constant minimal value at pH 4–9; after the addition of 5  $\mu\text{M}$  NaClO, the emission intensity at 505 nm was significantly increased. The pH independence of **BCIO** can be attributed to the fact that the lone pair of electrons on the pyrrole nitrogen takes part in the  $\pi$ -bonding system, thus making the protonation difficult.<sup>36</sup>

Evidence obtained from recent studies indicates that cancer cells, compared to normal cells, are under increased oxidative stress associated with oncogenic transformation, alterations in metabolic activity, and increased generation of ROS.<sup>3–5</sup> Thus, we tested whether **BCIO** is sensitive enough to determine the difference in the basal HClO levels between cancer and normal cells (Figure 2). After incubation of cancer cells (MCF-7 and

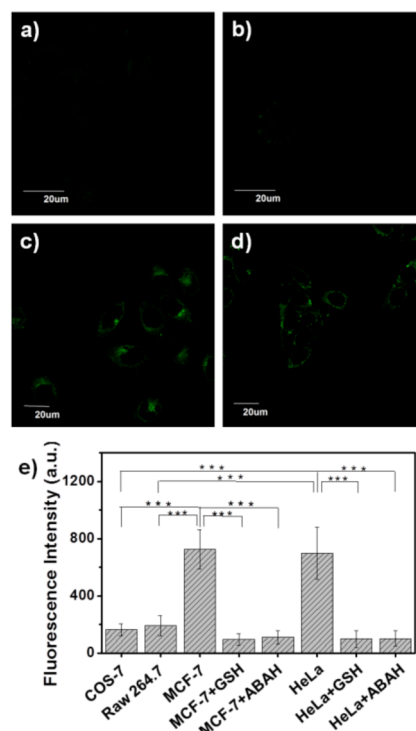


**Figure 2.** Fluorescence images of normal and cancer cells after incubation with 1  $\mu\text{M}$  **BCIO** for 20 min: (a) COS-7 cells, (b) raw 264.7 macrophages, (c) MCF-7 cells, and (d) HeLa cells. Images were acquired by using excitation and emission windows of  $\lambda_{\text{ex}} = 488 \text{ nm}$  and  $\lambda_{\text{em}} = 490\text{--}550 \text{ nm}$ , respectively. (e) Statistical analyses were performed with two-sample  $t$ -test ( $n = 10$  fields of cells). \*\*\* $P < 0.001$ , error bars are  $\pm$  sem.

HeLa) with **BCIO** for 20 min at 37  $^\circ\text{C}$ , **BCIO** penetrated the cell membranes and stained the cells with a clear fluorescence from the emission channel in the range 490–550 nm (Figure 2c,d). As shown in Figure S9, the emission maximum of **BCIO** (505 nm) in the cells was the same as that measured in PBS buffer solution. The fluorescence of **BCIO** was significantly reduced (Figure S10) by pretreating with glutathione (GSH, an important antioxidant within cells<sup>42</sup>) or 4-aminobenzoic acid hydrazide (ABAH, a potent inhibitor of MPO<sup>43</sup>). According to the linearity ( $F/F_0$  versus HClO concentration) established in Figure 1b and the quantification data (Figure 2e, where  $F_0$  is

the fluorescence intensity of **BCIO**+GSH/ABAH), the average basal HClO levels in MCF-7 and HeLa cells were estimated as ca. 9.45 and 8.23 nM, respectively. In the case of normal cell lines (COS-7 and Raw 264.7), almost no fluorescence (Figure 2a,b) was observed under the same conditions. Figure 2e showed that the fluorescence of **BCIO** in MCF-7 and HeLa cells was much stronger than that in COS-7 cells and Raw 264.7 macrophages ( $***P < 0.001$ ), demonstrating that **BCIO** could potentially be applied to differentiate between normal and cancer cells on the basis of their different basal HClO levels. Furthermore, the fluorescence intensity of **BCIO** significantly increased upon addition of NaClO in MCF-7 cells (Figure S11) or stimulation with lipopolysaccharide (LPS) and phorbol 12-myristate 13-acetate (PMA)<sup>44</sup> in Raw 264.7 macrophages (Figure S12), indicating that **BCIO** was capable of detecting changes in the HClO level in the presence of exogenous or endogenous HClO in live cells.

Elesclomol is an effective experimental ROS-generating anticancer agent<sup>9</sup> that displays selective sensitivity to breast cancer MCF-7 cells,<sup>45</sup> but the underlying molecular mechanism of action of elesclomol has not been elucidated in detail.<sup>46</sup> In this study, we employed **BCIO** to investigate whether HClO is generated during the elesclomol stimulation in MCF-7 cells. **BCIO**-prestained MCF-7 cells were treated with elesclomol, then the fluorescence images were recorded at different time points for 3 h (Figure 3a–f) and Figure 3g showed the plot of relative fluorescence intensity of **BCIO** against time. The

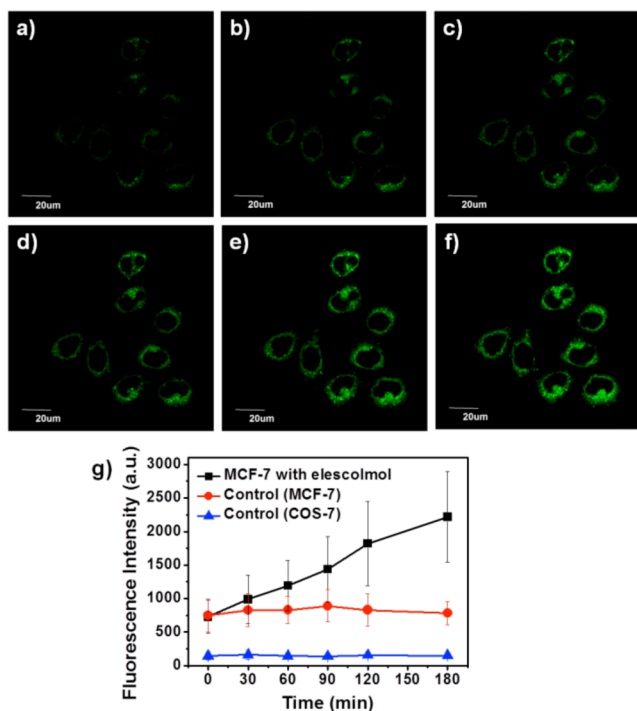


**Figure 3.** Time-dependent HClO generation induced by elesclomol in live MCF-7 cells. Cells were cultured with 1  $\mu$ M **BCIO** for 20 min, and then confocal fluorescence images were recorded after the addition of elesclomol (2  $\mu$ M) at different time points: (a) 0, (b) 30, (c) 60, (d) 90, (e) 120, and (f) 180 min. Images were acquired by using excitation and emission windows of  $\lambda_{\text{ex}} = 488$  nm and  $\lambda_{\text{em}} = 490$ –550 nm, respectively. (g) Plots of relative fluorescence intensities of **BCIO** against time: with elesclomol in MCF-7 (squares, black line), without elesclomol in MCF-7 (circles, red line), and with elesclomol in COS-7 (triangles, blue line).

fluorescence signal of **BCIO** significantly increased from  $726 \pm 244$  at 0 min to  $2217 \pm 677$  at 180 min, indicating that the addition of elesclomol caused time-dependent fluorescence enhancement. However, the fluorescence intensity of **BCIO** remained almost constant in the control sample without elesclomol (Figure S13), demonstrating that the observed changes in **BCIO** fluorescence could be attributed to the HClO generation induced by elesclomol in cancer cells. For any cancer therapeutics, the ability to selectively target tumors by exploiting the fundamental differences between normal and cancer cells represents a promising approach.<sup>46</sup> In another comparative experiment using COS-7 cells, much lower and almost unchanged emission intensities were observed during the elesclomol stimulation (Figure S14), indicating that the cellular oxidative stress induction did not occur in the nontransformed cells.

The MTT (3-(4,5-dimethylthiazol-2-yl)-2,5-diphenyltetrazolium bromide) tests showed that, after 24 h of cellular internalization of 1  $\mu$ M probe, more than 98% of the cells remained viable (Figure S15), indicating the low cytotoxicity of **BCIO**.

In conclusion, we synthesized **BCIO** by a Michael addition reaction of acryloyl chloride with 2, 4-dimethylpyrrole. **BCIO** functions as a HClO-specific fluorescent indicator that features a fast (within 1 s) and ultrasensitive response. The detection limit is as low as 0.56 nM, which is the highest sensitivity achieved to date. The pyrrole group at the *meso* position has an “enhanced PET” effect on the BODIPY fluorophore, so as to obtain the low background fluorescence and high signal-to-noise ratio. Significantly, **BCIO** can be applied to image basal HClO in cancer cells for the first time and monitor the time-dependent elevation of HClO caused by elesclomol in MCF-7 cells. It is therefore believed that **BCIO** provides a promising chemical tool for the study of HClO in tumor biology and the molecular understanding of the mechanism of action of elesclomol. Such work on developing ratiometric, NIR, and organelle/protein-targeted fluorescent probes based on **BCIO** is ongoing.

## ■ ASSOCIATED CONTENT

### 📄 Supporting Information

Synthesis, additional spectroscopic and imaging data, Gaussian calculation results, and MTT results. This material is available free of charge via the Internet at <http://pubs.acs.org>.

## ■ AUTHOR INFORMATION

### Corresponding Authors

fanjl@dlut.edu.cn

pengxj@dlut.edu.cn

### Notes

The authors declare no competing financial interest.

## ■ ACKNOWLEDGMENTS

This work was financially supported by NSF of China (21136002, 21376039, 21422601, and 21421005), National Basic Research Program of China (2013CB733702), Ministry of Education (NCET-12-0080), and Liaoning NSF (2013020115).

## ■ REFERENCES

- (1) Pelicano, H.; Carney, D.; Huang, P. *Drug Resist. Updates* **2004**, *7*, 97.

- (2) Schumacker, P. T. *Cancer Cell* **2006**, *10*, 175.
- (3) Toyokuni, S.; Okamoto, K.; Yodoi, J.; Hiai, H. *FEBS Lett.* **1995**, *358*, 1.
- (4) Hileman, E.; Liu, J.; Albitar, M.; Keating, M.; Huang, P. *Cancer Chemother. Pharmacol.* **2004**, *53*, 209.
- (5) Behrend, L.; Henderson, G.; Zwacka, R. M. *Biochem. Soc. Trans.* **2003**, *31*, 1441.
- (6) Kong, Q.; Lillehei, K. O. *Med. Hypotheses* **1998**, *51*, 405.
- (7) Kong, Q.; Beel, J. A.; Lillehei, K. O. *Med. Hypotheses* **2000**, *55*, 29.
- (8) Fruehauf, J. P.; Meyskens, F. L. *Clin. Cancer Res.* **2007**, *13*, 789.
- (9) Kirshner, J. R.; He, S.; Balasubramanyam, V.; Kepros, J.; Yang, C.-Y.; Zhang, M.; Du, Z.; Barsoum, J.; Bertin, J. *Mol. Cancer Ther.* **2008**, *7*, 2319.
- (10) Harrison, J. E.; Schultz, J. J. *Biol. Chem.* **1976**, *251*, 1371.
- (11) Winterbourn, C. C. J. *Clin. Invest.* **1986**, *78*, 545.
- (12) Weitzman, S. A.; Gordon, L. I. *Blood* **1990**, *76*, 655.
- (13) Klebanoff, S. J. *J. Leukocyte Biol.* **2005**, *77*, 598.
- (14) Aratani, Y.; Koyama, H.; Nyui, S.-i.; Suzuki, K.; Kura, F.; Maeda, N. *Infect. Immun.* **1999**, *67*, 1828.
- (15) Chen, X.; Tian, X.; Shin, I.; Yoon, J. *Chem. Soc. Rev.* **2011**, *40*, 4783.
- (16) Chen, X.; Wang, X.; Wang, S.; Shi, W.; Wang, K.; Ma, H. *Chem.—Eur. J.* **2008**, *14*, 4719.
- (17) Panizzi, P.; Nahrendorf, M.; Wildgruber, M.; Waterman, P.; Figueiredo, J.-L.; Aikawa, E.; McCarthy, J.; Weissleder, R.; Hilderbrand, S. A. *J. Am. Chem. Soc.* **2009**, *131*, 15739.
- (18) Yuan, L.; Lin, W.; Song, J.; Yang, Y. *Chem. Commun.* **2011**, *47*, 12691.
- (19) Kim, T.-I.; Park, S.; Choi, Y.; Kim, Y. *Chem.—Asian J.* **2011**, *6*, 1358.
- (20) Zhou, Y.; Li, J.-Y.; Chu, K.-H.; Liu, K.; Yao, C.; Li, J.-Y. *Chem. Commun.* **2012**, *48*, 4677.
- (21) Yuan, L.; Lin, W.; Xie, Y.; Chen, B.; Song, J. *Chem.—Eur. J.* **2012**, *18*, 2700.
- (22) Lou, Z.; Li, P.; Pan, Q.; Han, K. *Chem. Commun.* **2013**, *49*, 2445.
- (23) Lou, Z.; Li, P.; Song, P.; Han, K. *Analyst* **2013**, *138*, 6291.
- (24) Liu, F.; Wu, T.; Cao, J.; Zhang, H.; Hu, M.; Sun, S.; Song, F.; Fan, J.; Wang, J.; Peng, X. *Analyst* **2013**, *138*, 775.
- (25) Kenmoku, S.; Urano, Y.; Kojima, H.; Nagano, T. *J. Am. Chem. Soc.* **2007**, *129*, 7313.
- (26) Shepherd, J.; Hilderbrand, S. A.; Waterman, P.; Heinecke, J. W.; Weissleder, R.; Libby, P. *Chem. Biol.* **2007**, *14*, 1221.
- (27) Sun, Z.-N.; Liu, F.-Q.; Chen, Y.; Tam, P. K. H.; Yang, D. *Org. Lett.* **2008**, *10*, 2171.
- (28) Yang, Y.-K.; Cho, H. J.; Lee, J.; Shin, I.; Tae, J. *Org. Lett.* **2009**, *11*, 859.
- (29) Koide, Y.; Urano, Y.; Hanaoka, K.; Terai, T.; Nagano, T. *J. Am. Chem. Soc.* **2011**, *133*, 5680.
- (30) Chen, G.; Song, F.; Wang, J.; Yang, Z.; Sun, S.; Fan, J.; Qiang, X.; Wang, X.; Dou, B.; Peng, X. *Chem. Commun.* **2012**, *48*, 2949.
- (31) Xu, Q.; Lee, K.-A.; Lee, S.; Lee, K. M.; Lee, W.-J.; Yoon, J. *J. Am. Chem. Soc.* **2013**, *135*, 9944.
- (32) Cheng, G.; Fan, J.; Sun, W.; Sui, K.; Jin, X.; Wang, J.; Peng, X. *Analyst* **2013**, *138*, 6091.
- (33) Wu, X.; Li, Z.; Yang, L.; Han, J.; Han, S. *Chem. Sci.* **2013**, *4*, 460.
- (34) Manjare, S. T.; Kim, J.; Lee, Y.; Churchill, D. G. *Org. Lett.* **2013**, *16*, 520.
- (35) Liu, S.-R.; Wu, S.-P. *Org. Lett.* **2013**, *15*, 878.
- (36) Wade, L. G. Jr. In *Organic Chemistry*, 8th ed.; Jaworski, A., et al., Eds.; Pearson Education, Inc.: New York, 2013; p 732.
- (37) de Silva, A. P.; Gunnlaugsson, T.; Rice, T. E. *Analyst* **1996**, *121*, 1759.
- (38) Callan, J. F.; de Silva, A. P.; Magri, D. C. *Tetrahedron* **2005**, *61*, 8551.
- (39) Manjare, S. T.; Kim, S.; Heo, W. D.; Churchill, D. G. *Org. Lett.* **2013**, *16*, 410.
- (40) Yu, F.; Li, P.; Li, G.; Zhao, G.; Chu, T.; Han, K. *J. Am. Chem. Soc.* **2011**, *133*, 11030.
- (41) Yu, F.; Li, P.; Wang, B.; Han, K. *J. Am. Chem. Soc.* **2013**, *135*, 7674.
- (42) Schafer, F. Q.; Buettner, G. R. *Free Radic. Biol. Med.* **2001**, *30*, 1191.
- (43) Kettle, A. J.; Gedye, C. A.; Winterbourn, C. C. *Biochem. J.* **1997**, *321*, 503.
- (44) Gomez-Mejiba, S. E.; Zhai, Z.; Gimenez, M. S.; Ashby, M. T.; Chilakapati, J.; Kitchin, K.; Mason, R. P.; Ramirez, D. C. *J. Biol. Chem.* **2010**, *285*, 20062.
- (45) Alli, E.; Ford, J. M. *DNA Repair* **2012**, *11*, 522.
- (46) Nagai, M.; Vo, N. H.; Shin Ogawa, L.; Chimmanamada, D.; Inoue, T.; Chu, J.; Beaudette-Zlatanova, B. C.; Lu, R.; Blackman, R. K.; Barsoum, J.; Koya, K.; Wada, Y. *Free Radic. Biol. Med.* **2012**, *52*, 2142.